

# METALLOGRAPHIC EVALUATION OF THE WELDABILITY OF HIGH STRENGTH ALUMINIUM ALLOYS USING FRICTION SPOT WELDING

J. Vercauteren<sup>1</sup>, K. Faes<sup>2</sup> and W. De Waele<sup>3</sup>

<sup>1</sup> Ghent University, Belgium

<sup>2</sup>The Belgian Welding Institute, Belgium

<sup>3</sup>Ghent University, Laboratory Soete, Belgium

**Abstract:** Friction spot welding is a recent solid-state welding technique well suited for spot-joining lightweight materials in overlap condition. Aerospace and transport industries show great interest in this technique to join high-strength aluminium alloys, but published research is still limited. In this project, the link between process parameters and weld quality is investigated for EN AW-7075-T6 material. Techniques used are metallographic qualification, measurement of hardness reduction and lap shear strength. This paper focusses on the metallographic investigation of the weld region and its imperfections. Increasing joining time and heat input creates an easier material flow resulting in fewer imperfections. Limited plunge depths lead to typical interface imperfections. Variation in the rotational speed shows distinctive stir zone shapes as a consequence of severe stirring and frictional heat.

**Keywords:** Friction spot welding, EN AW-7075-T6, metallography, microstructure

## 1 INTRODUCTION

High strength lightweight materials, such as some aluminium alloys, gain importance in industry, especially in automotive and aeronautic fields [1-3]. Joining of these materials is an important step in the production of components or structures. Many joining techniques exist such as fusion welding, riveting, bolting, etc. Nevertheless, researchers keep looking for more efficient alternative techniques as each joining technology has its disadvantages [4]. Fusion welds can for example contain imperfections which deteriorate the mechanical strength of the bond. Furthermore, some high strength lightweight alloys suffer from low weldability issues [5]. Moreover, aluminium alloys are good thermal conductors which means that supplied heat rapidly distributes throughout the specimen. Keeping the specimen above the melting temperature thus requires a high energy input. Mechanical fasteners add non-negligible mass to the structure which is undesirable in lightweight applications.

Friction welding offers a solution to most of the issues concerning lightweight materials. This work focuses on the friction spot welding (FSpW) process, also referred to as refill friction stir spot welding (refill FSSW). It is part of a collective international research project called INNOJOIN [6], an acronym for innovative joining. FSpW is a solid-state welding process well suited for spot-joining lightweight materials in overlap configuration. It differs from the friction stir spot weld (FSSW) process in the ability to refill the keyhole and hence eliminates its major disadvantages: stress concentration and corrosion at the keyhole. Friction spot welding is seen as a green manufacturing method because no additional filler material is required and there is no waste material [4,7]. The welding process has potential for mass production lines as the welding time is relatively short and the process can be automated easily.

The overall goal of this work is the evaluation of the weldability of high-strength aluminium alloys using friction spot welding. In previous work [8] the weldability of alloy EN AW-7475-T761 has been evaluated; this study focuses on aluminium alloy EN AW-7075-T6. This paper mainly focusses on the metallographic investigation and aims to link the most important process parameters to the quality of the weld regarding imperfections.

## 2 FRICTION SPOT WELDING

### 2.1 Process description

The friction spot welding process is a solid-state spot joining technology to join sheets in overlap condition. The solid-state property implies that the working temperature does not exceed the melting temperature of the materials. The joint is fully generated by frictional heat and plastic work whereby a metallurgical bond is formed. FSpW is a rather recent technique as it was invented by the GKSS research centre in 1999 [9].

The non-consumable tool consists of three components: a concentric clamping ring, sleeve and pin. All three components can act independently in the axial direction. The pin and sleeve can rotate about their axis in the same direction. The function of the clamping ring is to fix the sheets rigidly in overlap configuration against a backing anvil while the welding process takes place.

The four process stages are depicted in Figure 1. In the first stage, the clamping ring fixes the plates while the pin and sleeve start rotating against the upper plate. As from the second stage the sleeve plunges into the material while rotating at high rotational speed. The pin rises, creating a cavity of the exact required volume for the plasticised material. The sleeve displaces the material underneath and forces it into the cavity provided by the pin rise. Between the second and third stage, the sleeve reaches a pre-defined depth. The frictional heat and mechanical work delivered by the stirring, bond the sheets at their interface. In the third stage, tool and sleeve translation reverse. The plasticised material that accumulated under the pin is pushed back in the keyhole created by the sleeve plunging. When retracting the complete tool in stage four, a flat surface appears. A typical surface view of such a spot weld is shown in Figure 2. Three concentric rings originating from contact with clamping ring, sleeve and pin are clearly visible.

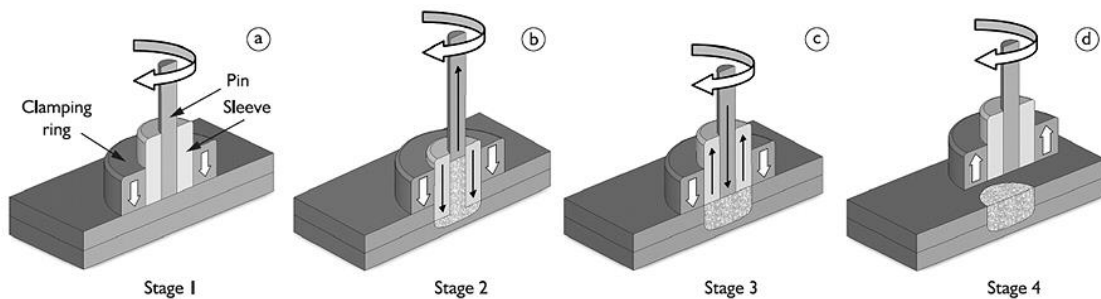


Figure 1: Friction spot welding stages [10]

The process, and thus the weld quality, is controlled by several welding parameters. This work focuses on three parameters: rotational speed, plunge depth and joining time.

The rotational speed (RS) of the pin and sleeve controls the material flow. The upper value is limited by the machine capacity, while the lower value is restricted by a minimum required heat input. The amount of heat input determines the softening of the workpiece. The softer the material, the easier the tool can plunge in. However, this also results in a wider heat affected zone around the weld nugget. A critical, and very material dependent parameter is the plunge depth (PD) [11]. This is the maximum depth the sleeve plunges into the material measured from the top surface of the upper sheet. The plunge depth is often chosen such that the sleeve plunges in the lower sheet for about 25-30 % of the lower plate thickness. This is in good agreement with the common practice in FSW [12]. A third process parameter is the joining time (JT) which consists of three sub-parameters: plunge time (PT), dwell time (DT) and retraction time (RT). These time parameters are graphically visualized in Figure 3. The joining time influences the amount of heat input, the plunge time and retraction time determine the rate of plastic deformation of the weld zone. Related parameters are the plunge rate (PR) and retraction rate (RR).

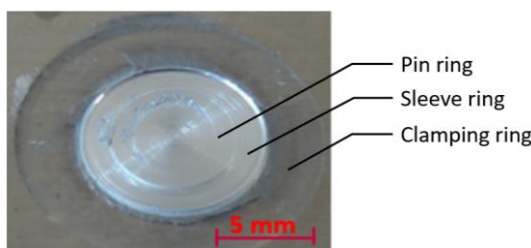


Figure 2: Typical appearance of a friction spot weld in EN AW-7475-T761 [13]

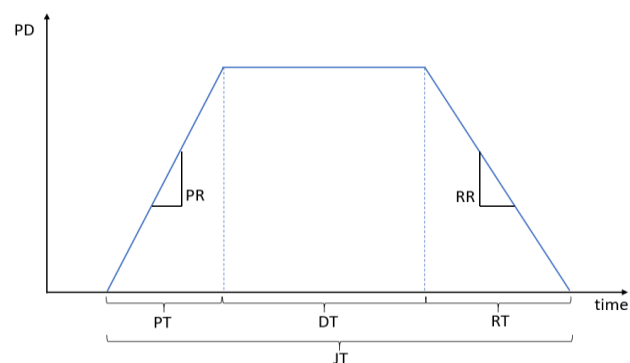


Figure 3: Plunge depth over time and the different time parameters

## 2.2 Weld cross-section

A friction spot weld consists of different microstructural regions, called weld zones. Figure 4 shows the stir zone (SZ) and the thermo-mechanically affected zone (TMAZ). A third weld zone, the heat-affected zone (HAZ), is not clearly visible on the optical microscope image. All weld zones differ in microstructure and mechanical properties from the base material (BM) as a result of the welding process. The SZ is the centre of the weld and has approximately the same width as the sleeve diameter. It is characterized by refined and equiaxed grains as a result of dynamic recrystallization. This is the effect of the high strain rate and the high local temperatures during the stirring process [14]. Next to the SZ, the TMAZ exists as a transitional region between the SZ and the HAZ. This zone is formed by moderate deformations and temperatures. The microstructure is characterized by elongated and deformed grains caused by the material flow [15]. As the TMAZ is a transition region, it is hard to define the boundaries. The HAZ is the first zone that is not affected by plastic deformations. As the name suggests, the microstructure of this zone is influenced by the conducted heat from the welding process. Grain growth has occurred due to the thermal treatment, but the exact boundary between the TMAZ and the HAZ is difficult to localise microscopically. Far enough from the weld centre, all effects from the welding process on the microstructure disappear. This is where the HAZ ends and the BM starts.

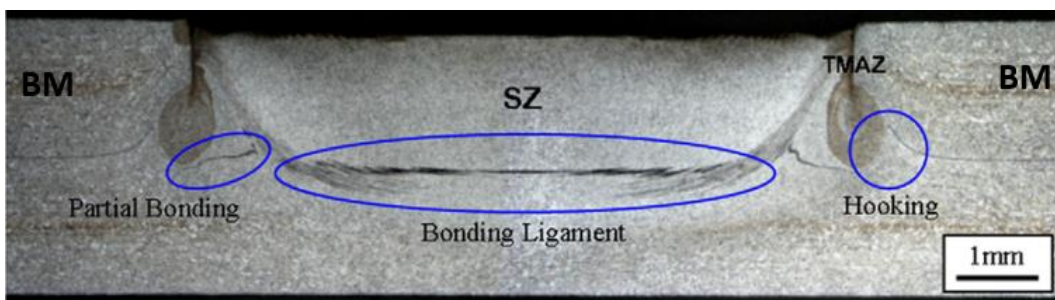


Figure 4: Typical cross-section of a FSpW weld in EN AW-6181-T4 [15].

Three geometrical features are often reported in metallographic inspection: hooking, partial bonding and bonding ligament. The location and appearance of these geometrical features are indicated in Figure 4. The hook feature is a transitional zone between the completely bonded regions and separated interfaces. It is suggested that its formation arises from the plastic upward bending of the interface due to tool penetration into the lower sheet. The importance of hooking lies in the fact that tensile shear strength of a joint decreases monotonically with increasing hook height [16]. The bonding ligament is a region of good adhesion between the upper and lower sheet material [15]. It is located underneath the stir zone and forms the strongest metallurgical bond in the weld. Tier et al. [11] showed that a longer, flatter and stronger bonding ligament can be obtained in EN AW-5042-O for lower rotational speeds. For larger rotational speed, the bonding ligament is curved upwards and the effective bonding ligament length is smaller. However, the presence of the bonding ligament is not always visible in all materials. Finally, the partial bonding zone is a transition region between the hooking and the bonding ligament with minor bonding strength.

Apart from the features described above, imperfections related to improper welding parameter combinations can occur such as lack of mixing, void inclusions or incomplete refill. All these imperfections are located along the path of the sleeve plunge and thus associated with the material flow. Incomplete refill can be partly assigned to the extrusion of material into the tolerance gap between the clamping ring and the sleeve [17].

## 3 EXPERIMENTAL STUDY

### 3.1 Material and equipment

In the present investigation, overlap joints were produced using sheets in the aluminium alloy EN AW-7075-T6, which is often used for aerospace applications. The sheets had a thickness of 1.6 mm. The chemical composition of the alloy is given in Table 1.

Table 1: Typical chemical composition of EN AW-7075-T6 in weight % [18]

| Al        | Cr        | Cu    | Fe    | Mg      | Mn    | Si    | Ti    | Zn      | Other  |
|-----------|-----------|-------|-------|---------|-------|-------|-------|---------|--------|
| 87.2-91.4 | 0.18-0.28 | 1.2-2 | 0-0.5 | 2.1-2.9 | 0-0.3 | 0-0.4 | 0-0.2 | 5.1-6.1 | 0-0.15 |

The experiments were performed using commercial friction spot welding equipment RPS 100 (Harms & Wende, Germany). The welding machine is equipped with a main head, which contains the welding tool. The clamping ring, sleeve and pin have an outer diameter of respectively 14.5, 9.0 and 6.0 mm. The machine is capable of applying axial forces up to 15 kN and rotational speeds up to 3300 rpm. Both the pin and the sleeve are provided with several circumferential grooves. This is done to enhance the material flow during the process [11].

### 3.2 Measurements

Welds in overlap configuration are produced with different process parameter combinations. After welding, a longitudinal section through the centre of the weld nugget was embedded, ground and polished to investigate using an Olympus MX51 optical microscope. Each sample is first inspected in the non-etched condition as this facilitates the detection of imperfections. The total area percentage of imperfections in the cross-section is calculated afterwards. Figure 5 shows a non-etched cross section with several imperfections and a coloured version with detected imperfections in red. The total area percentage of imperfections is calculated as the percentage red of the complete rectangle. Only imperfections with a minimum area of 0.002 square millimetres are taken into account. The global percentage of imperfections gives an indication of the overall weld quality, but neglects that some imperfections are more dangerous than others. Sharp, fine imperfections like a non-bonded interface lead to higher stress concentrations than spherical voids. Additional measurements were performed on two types of imperfections: the depth of the incomplete refill and the width of the non-bonded interface.

Sequentially, the samples were etched using Keller's reagent to reveal the weld microstructure. Different regions were inspected in detail.

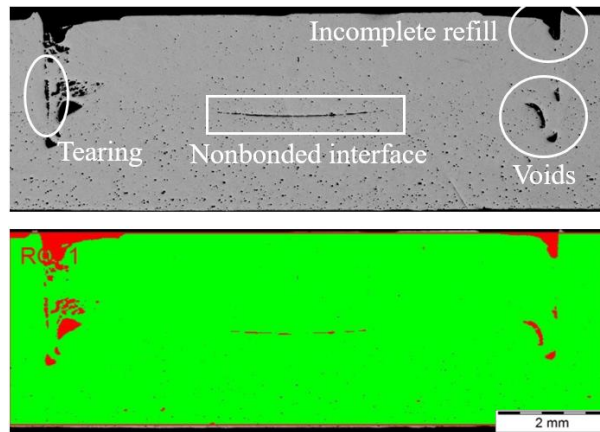


Figure 5: Non-etched cross-section (top) and area percentage of imperfections (bottom)

### 3.3 Overview of the experiments

The three main process parameters (rotational speed, plunge depth and joining time) were varied on three levels. An overview of the values is given in Table 2. All 27 possible combinations were investigated by metallographic inspection. Plunge rate and retraction rate were kept constant at a rate of 0.8 mm/s. Dwell time follows from the predefined joining time. Clamp pressure was fixed at a level of 3.5 bar.

Table 2: Parameter combinations

|          |                    |
|----------|--------------------|
| RS (rpm) | 1000 – 2000 – 3000 |
| PD (mm)  | 1.6 – 2.0 – 2.4    |
| JT (s)   | 6 – 8 – 10         |

## 4 RESULTS

### 4.1 Influence of joining time

The joining time is closely related to the amount of heat input into the weld. Recall that the total joining time consists of three different parts. Increasing the joining time without changing the other parameters is equivalent to increasing the dwell time of the tool. Figure 6 compares three (non-)etched cross-sections of welds produced at a rotational speed of 2000 rpm, a plunge depth of 1.6 mm and three different joining times of respectively 6, 8 and 10 s. For increasing joining time the incomplete refill imperfection disappears, leading to an almost perfect cross-section. However, it is important to notice that the weld combination at the middle (JT = 8s) contains a non-bonded interface which is probably more dangerous than the large incomplete refill



imperfection in the upper weld. The etched stir zone becomes darker for longer welding times, indicating a finer grain size at the nugget centre. The recrystallized zone also reaches deeper into the lower sheet, although the plunge depth is unchanged. These are consequences of the increased heat input.

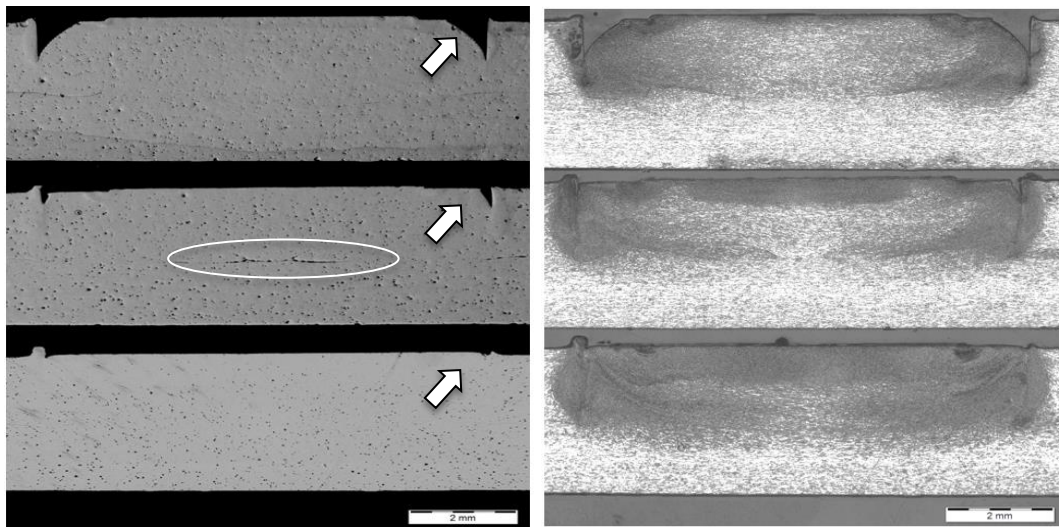


Figure 6: Varying joining time: 6 s (top), 8 s (middle), 10 s (bottom)

The influence of the joining time as illustrated in Figure 6 is a global effect throughout all weld samples. Figure 7 and Figure 8 show imperfection measurements at different joining times and rotational speeds. Measurement points at the same rotational speed and joining time differ in plunge depth, no replications were made. The measurements show a large variation and therefore a dashed trendline of mean values is added to the graphs. It is clear that overall both the total area percentage of imperfections and the depth of incomplete refill decrease with increasing the joining time. Especially the improvement from 6 s to 8 s joining time is significant. Only the parameter combination at the lowest rotational speed (RS=1000 rpm) and the shortest joining time (JT=6 s) does not correspond with the overall trend.

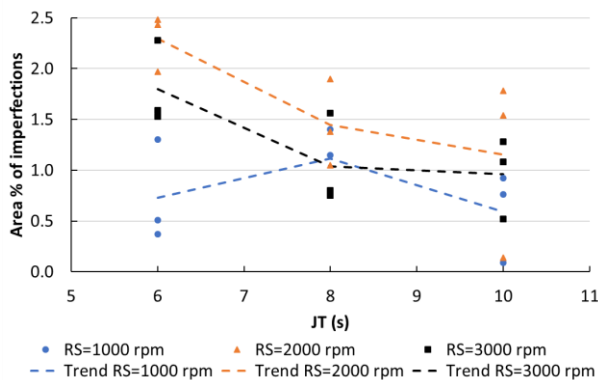


Figure 7: Mean area % of imperfections at varying JT

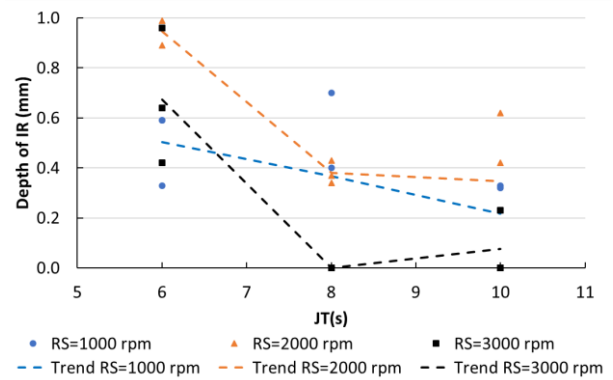


Figure 8: Mean depth of IR at varying JT

#### 4.2 Influence of plunge depth

The plunge depth was varied starting from the upper plate thickness (1.6 mm) up to 50% into the lower plate (2.4 mm). From the experiments, it seems that the plunge depth of 1.6 mm is prone to imperfections at the sheet interface. The absence of the tool penetration into the lower plate does not create a strong interface bond. Welds containing non-bonded interfaces and partial bonding features were always produced with this low plunge depth. Figure 9 shows at the left a non-bonded interface at the centre of the stir zone. This sharp and narrow imperfection can be detrimental in lap shear loading. At the right, a partial bonding is displayed. The wrinkling line starts from the separated surfaces outside the weld nugget and penetrates into the stir zone. On the same picture, a void along the sleeve path is visible. Hooking features were discovered in the stir zone for some of the welds produced at the smallest plunge depth. Figure 10 shows two hook features inside the stir zone. The lower one originates from the sheet interface and is formed during the plastic deformation of the lower plate. The upper hook is formed during the refilling stage. The void in the corner of the weld shows that the keyhole of the sleeve is not properly refilled. For deeper plunge depths, the hook

never reaches into the weld nugget. A slight decrease in voids is observed for deeper plunge depths, but this influence is not significant.

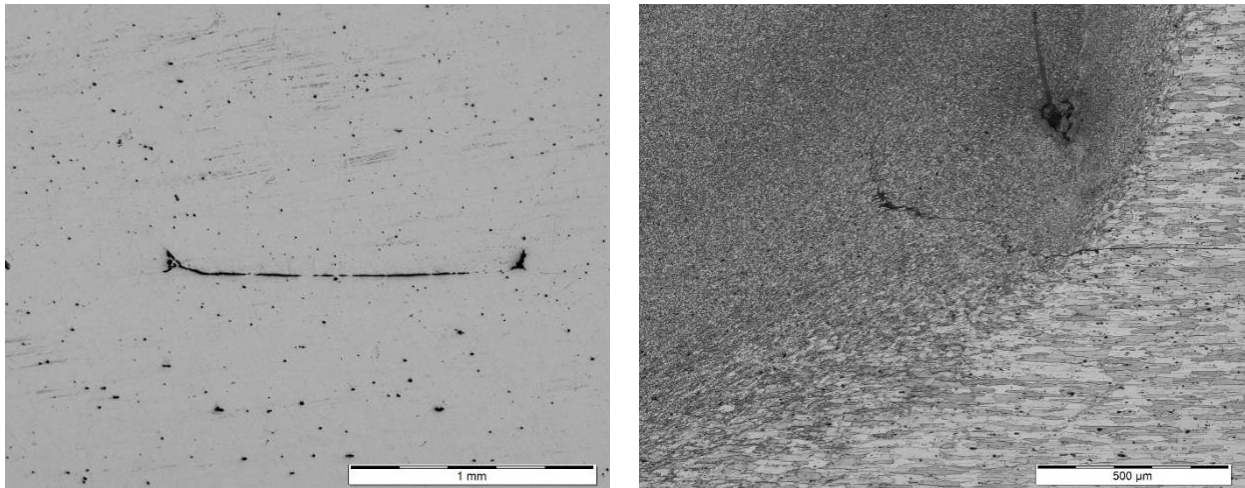


Figure 9 Non-bonded interface (left) and partial bonding (right) at a plunge depth of 1.6 mm

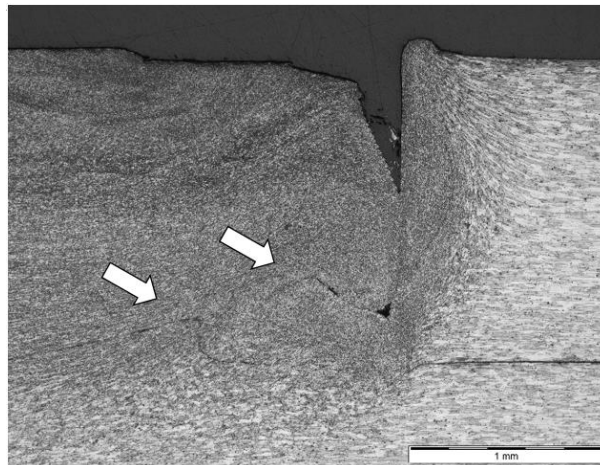


Figure 10: Hook features at a plunge depth of 1.6 mm

### 4.3 Influence of rotational speed

Figure 11 shows three etched cross-sections of welds produced with a joining time of 8 s, a plunge depth of 2 mm and three varying rotational speeds. The difference in shape and size of the stir zone is very distinctive. At lower rotational speed, the affected zone is curved and reaches much deeper than the plunge depth. At high rotational speed, the stir zone depth is rectangular and limited to the plunge depth. Furthermore, the grains are finer at low rotational speed, with only a vertical zone of coarse grains right underneath the pin zone. At the centre of the pin, the circumferential velocity is zero and the least amount of stirring takes place. At higher rotational speed, horizontal bands of fine grains become visible. The reason for this difference is not yet completely understood. FSpW machine data showed that 60% more torque was required to produce a weld at 1000 rpm compared with welds at 2000 and 3000 rpm, indicating a higher coefficient of friction between tool and workpiece. It is not recommended to weld at 1000 rpm when the machine is in a cold state as this has led to overcurrent warnings of the spindle.

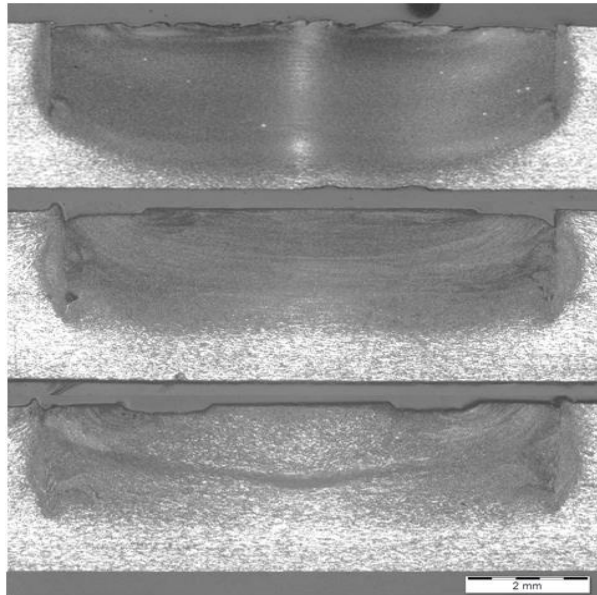


Figure 11: Varying RS: 1000 rpm (top), 2000 rpm (middle) and 3000 rpm (bottom)

In [19], effects of rotational speed on the microstructure and mechanical properties of friction stir welded 7075-T6 Al alloys were investigated. It was found that with increasing the rotational speed, higher peak temperatures and grain coarsening were present. Higher strain rates result in fine recrystallized grains, but higher temperatures improve the grain growth of the recrystallized grains [19]. It is a trade-off between these two effects that determines the final grain size.

As the rotational speed is closely related to the material flow, it has a significant effect on the amount of imperfections. Figure 12 and Figure 13 show the influence of the rotational speed in a similar way as for the joining time in section 4.1. In both graphs, welds with a rotational speed of 2000 rpm perform worst. The incomplete refill imperfection is smallest at the highest rotational speed combined with medium to long joining times, as a result of excessive stirring and a fluent material flow. On both graphs, the earlier discussed influence of the joining time on imperfection size is again visible.

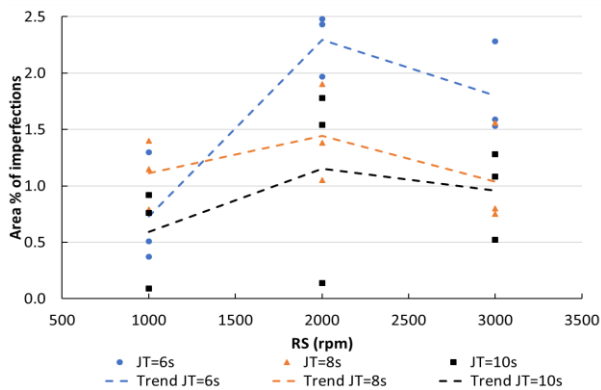


Figure 12: Mean area % of imperfections at varying RS

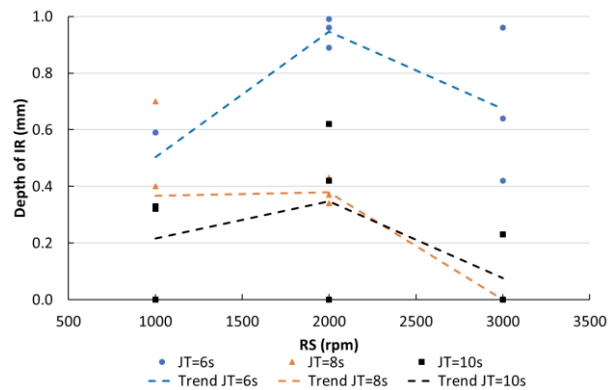


Figure 13: Mean depth of IR at varying RS

## 5 CONCLUSIONS

FSpW is a recent solid-state joining technique with a lot of potential. This work studied the effect of three main welding parameters (JT, PD and RS) on the metallographic quality of the weld cross-section. Lap joints were produced in 1.6 mm EN AW-7075-T6 aluminium alloy. Overall imperfection percentage of the weld decreased for increasing joining time and thus heat input. Most imperfections were formed at a rotational speed of 2000 rpm, while the incomplete refill imperfection was minimal at a rotational speed of 3000 rpm. Low plunge depths, equal to the sheet thickness, should be avoided as this frequently results in imperfections at the interface such as non-bonded interfaces, partial bonding and hooking. Especially the rotational speed determines the final shape of the stir zone and its grain size. It is believed that a trade-off between dynamic recrystallization and grain growth is the cause of this phenomenon. The metallographic observations will be linked to mechanical properties as hardness and strength in next research steps.

## 6 ACKNOWLEDGEMENTS

The authors would like to acknowledge the support of the employees of the Belgian Welding Institute (BWI) for the metallographic training and support.

## 7 REFERENCES

- [1] F. Alshmiri, 'Lightweight Material: Aluminium High Silicon Alloys in The Automotive Industry', in *Advanced Technologies in Manufacturing, Engineering and Materials, Pts 1-3*, vol. 774–776, Y. H. Kim and P. Yarlagadda, Eds. Stafa-Zurich: Trans Tech Publications Ltd, 2013, pp. 1271–1276.
- [2] R. Dhingra and S. Das, 'Life cycle energy and environmental evaluation of downsized vs. lightweight material automotive engines', *J. Clean Prod.*, vol. 85, pp. 347–358, Dec. 2014.
- [3] K. Grigoriou and A. P. Mouritz, 'Comparative assessment of the fire structural performance of carbon-epoxy composite and aluminium alloy used in aerospace structures', *Mater. Des.*, vol. 108, pp. 699–706, Oct. 2016.
- [4] R. Rajan, P. Kah, B. Mvola, and J. Martikainen, 'Trends in Aluminium Alloy Development and Their Joining Methods', *Rev. Adv. Mater. Sci.*, vol. 44, no. 4, pp. 383–397, 2016.
- [5] T. Rosendo *et al.*, 'Mechanical and microstructural investigation of friction spot welded AA6181-T4 aluminium alloy', *Mater. Des.*, vol. 32, no. 3, pp. 1094–1100, Mar. 2011.
- [6] 'INNOJOIN: Development and evaluation of advanced welding technologies for multi-material design with dissimilar sheet metals | www.bil-ibs.be'. [Online]. Available: <http://www.bil-ibs.be/en/onderzoeksproject/innojoin-development-and-evaluation-advanced-welding-technologies-multi-material-d>. [Accessed: 27-Apr-2017].
- [7] T. Rosendo, M. Tier, J. Mazzaferro, C. Mazzaferro, T. R. Strohaecker, and J. F. Dos Santos, 'Mechanical performance of AA6181 refill friction spot welds under Lap shear tensile loading', *Fatigue Fract. Eng. Mater. Struct.*, vol. 38, no. 12, pp. 1443–1455, Dec. 2015.
- [8] T. Kolba, K. Faes, and W. De Waele, 'Experimental investigation of the weldability of high strength aluminium using friction spot welding'. [Online]. Available: <http://ojs.ugent.be/SCAD/article/view/3638>.
- [9] T. Montag, J.-P. Wulfsberg, H. Hameister, and R. Marschner, 'Influence of Tool Wear on Quality Criteria for Refill Friction Stir Spot Welding (RFSSW) Process', *Procedia CIRP*, vol. 24, pp. 108–113, Jan. 2014.
- [10] 'Friction spot welding | www.bil-ibs.be'. [Online]. Available: <http://www.bil-ibs.be/en/friction-spot-welding>. [Accessed: 02-Nov-2016].
- [11] M. D. Tier *et al.*, 'The influence of refill FSSW parameters on the microstructure and shear strength of 5042 aluminium welds', *J. Mater. Process. Technol.*, vol. 213, no. 6, pp. 997–1005, Jun. 2013.
- [12] M. A. D. Tier *et al.*, 'A Study About the Mechanical Properties of Alclad AA2024 Connections Processed by Friction Spot Welding 1', in *ResearchGate*, 2009.
- [13] O. Bilouet, 'Soudage par Friction Spot d'assemblages d'alliages d'aluminium', Mons, Belgique, Jan-2016.
- [14] A. Gerlich, G. Avramovic-Cingara, and T. H. North, 'Stir zone microstructure and strain rate during Al 7075-T6 friction stir spot welding', *Metall. Mater. Trans. A-Phys. Metall. Mater. Sci.*, vol. 37A, no. 9, pp. 2773–2786, Sep. 2006.
- [15] T. Rosendo *et al.*, 'Mechanical and microstructural investigation of friction spot welded AA6181-T4 aluminium alloy', *Mater. Des.*, vol. 32, no. 3, pp. 1094–1100, Mar. 2011.
- [16] J. Y. Cao, M. Wang, L. Kong, and L. J. Guo, 'Hook formation and mechanical properties of friction spot welding in alloy 6061-T6', *J. Mater. Process. Technol.*, vol. 230, pp. 254–262, Apr. 2016.
- [17] Y. Q. Zhao, H. J. Liu, S. X. Chen, Z. Lin, and J. C. Hou, 'Effects of sleeve plunge depth on microstructures and mechanical properties of friction spot welded alclad 7B04-T74 aluminum alloy', *Mater. Des.*, vol. 62, pp. 40–46, Oct. 2014.
- [18] *CES EduPack 2016*. Cambridge, UK: Granta Design Limited.
- [19] H. Rezaei and H. Bisadi, 'Effect of rotational speeds on microstructure and mechanical properties of friction stir-welded 7075-T6 aluminium alloy', *ournal of Mechanical Engineering Science*, vol. Proceedings of the Institution of Mechanical Engineers Part C, no. vols 203-210, Aug. 2011.